

Supplementary materials

Computational study of the post-transition state dynamics for the OH + CH₃OH reaction probed by photodetachment of the CH₃O⁻(H₂O) anion

Tatsuhiro Murakami ^{*,†,1,2} and Toshiyuki Takayanagi ^{‡,1}

¹Department of Chemistry, Saitama University, Shimo-Okubo 255, Sakura-ku, Saitama City, Saitama, 338-8570, Japan

²Department of Materials & Life Sciences, Faculty of Science & Technology, Sophia University, 7-1 Kioicho, Chiyoda-ku, Tokyo, 102-8554, Japan

Contents

S1 Figures and Tables for the supporting information

S2

^{*}Corresponding author

[†]E-mail: murakamit@mail.saitama-u.ac.jp, ORCID: 0000-0001-8904-8673

[‡]E-mail: tako@mail.saitama-u.ac.jp, ORCID: 0000-0003-0563-9236

S1 Figures and Tables for the supporting information

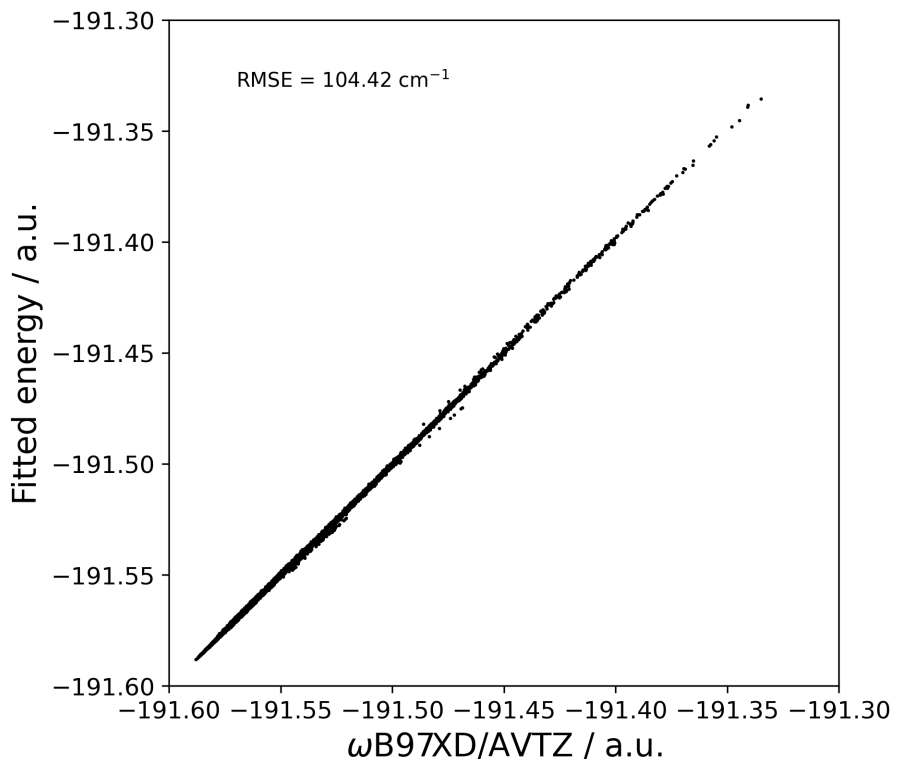


Figure S1: The potential energy fitted with respect to ω B97XD/AVTZ energy

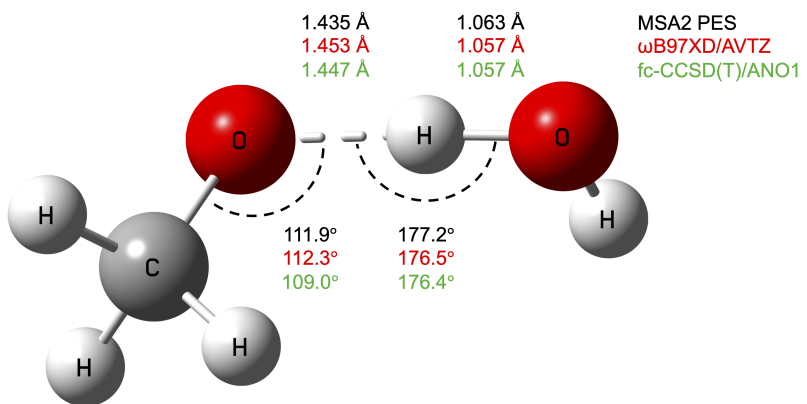


Figure S2: Comparison of the equilibrium geometry of the $\text{CH}_3\text{O}^-(\text{H}_2\text{O})$ anion. The geometric parameters in black, red, blue, and green correspond to the fitted PES, ω B97XD/aug-cc-pVTZ(AVTZ) outcomes, and the CCSD(T) results taken from Ref. 11, respectively.

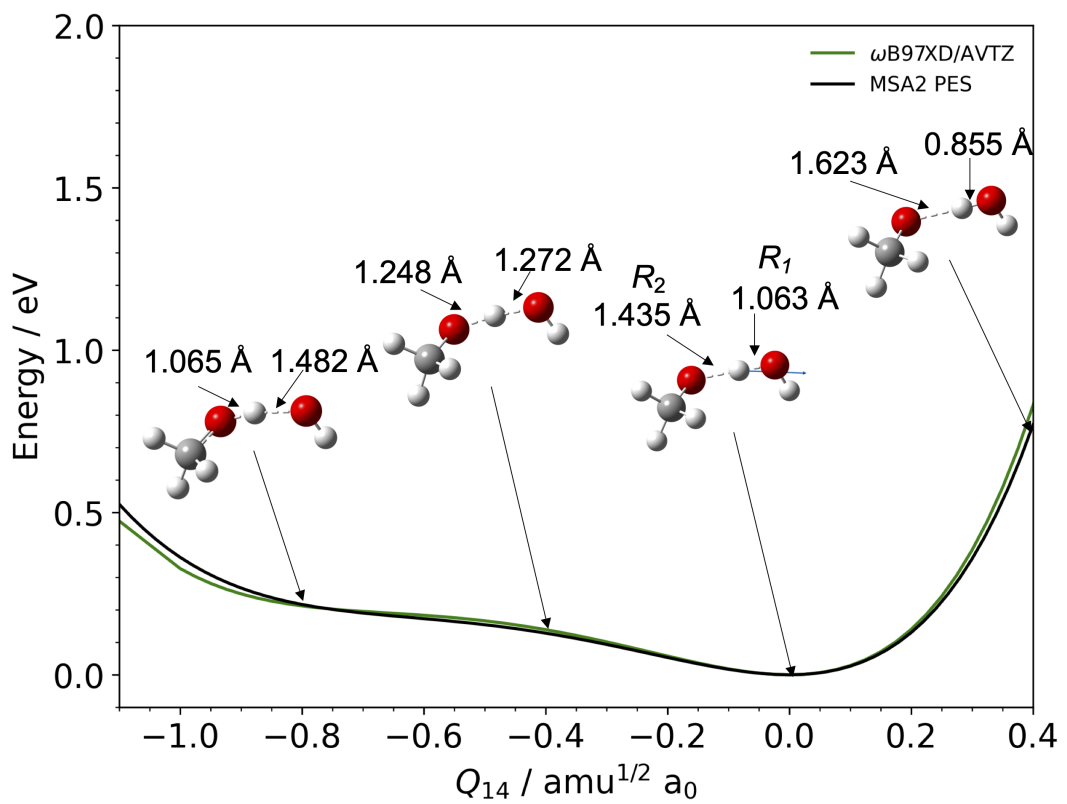


Figure S3: Potential energy curves of the MSA2 PES(black line) and the ω B97XD/aug-cc-pVTZ(AVTZ) PES (green line) along hydrogen transfer mode, Q_{14}

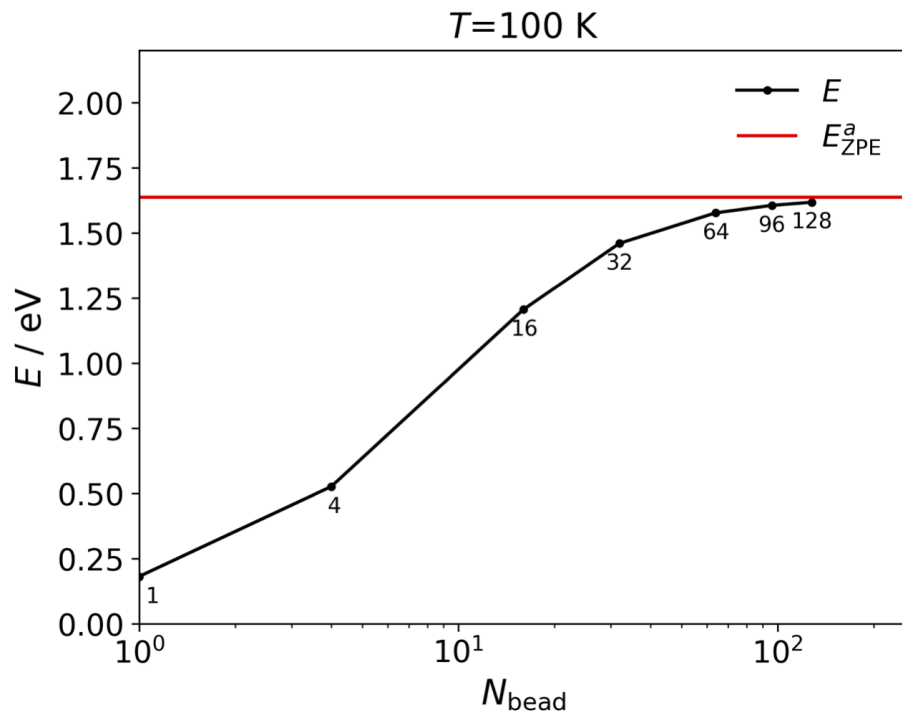


Figure S4: Convergence analysis of the number of beads at the temperature $T = 100$ K. Here, E denotes the internal energy of the anion system, while E_{ZPE}^a represents the zero-point vibrational energy.

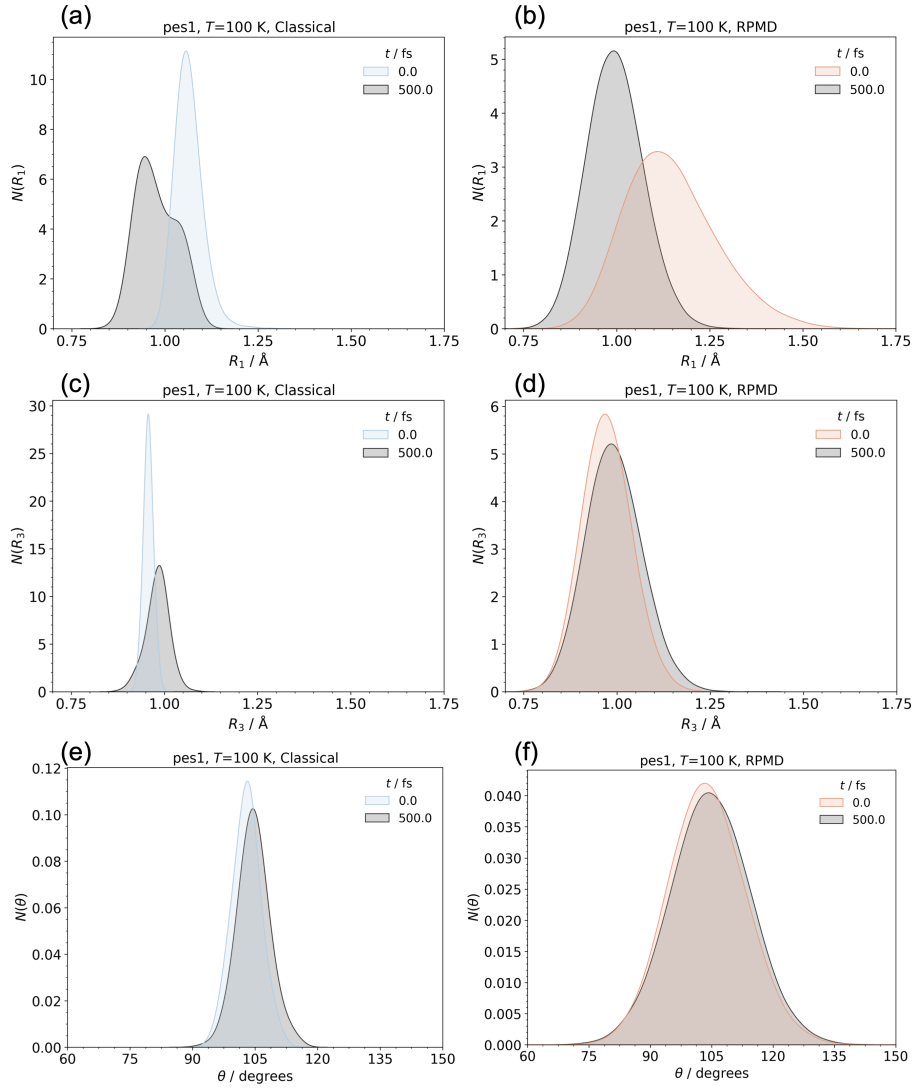


Figure S5: Time-dependent probability densities of (a) R_1 , (c) R_3 , and (e) θ at $t=0$ and 500 fs for classical MD, and (b) R_1 , (d) R_3 , and (f) θ at $t=0$ and 500 fs for RPMD on PES1.

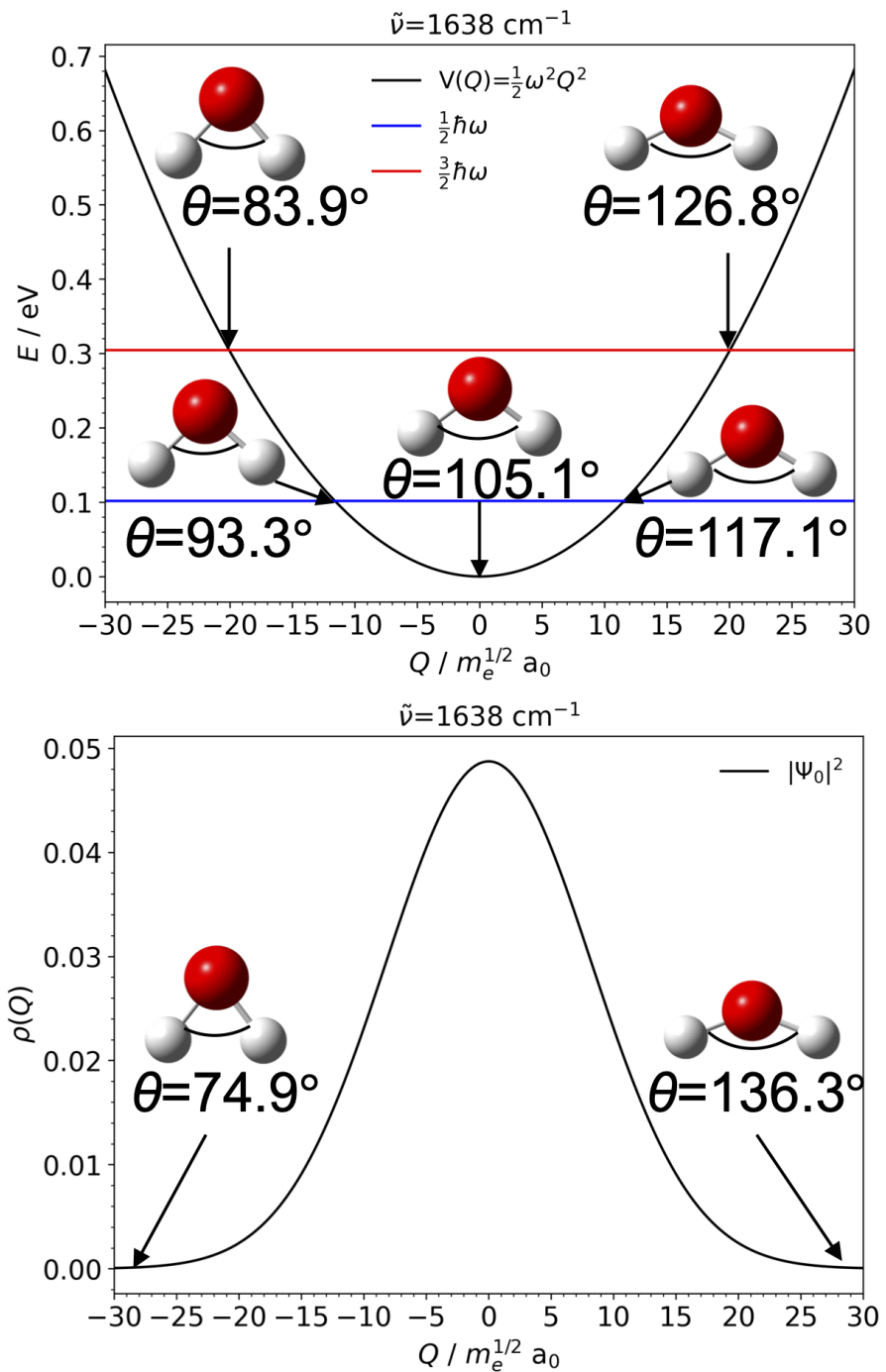


Figure S6: Harmonic potential curve (upper panel) and probability density of the zero-point wave function $|\Psi_0|^2$ for bending motion computed using the ω B97XD/aug-cc-pVTZ level of theory (lower panel), with bending angles at key geometries

Table S1: Relative energies (in eV) for the CH_3O^- (H_2O) anion equilibrium structure, $\text{CH}_3\text{OH} + \text{OH}^-$ and $\text{CH}_3\text{O}^- + \text{H}_2\text{O}$ fragments calculated by the $\omega\text{B97XD}/\text{AVTZ}$ and the mHEAT-345(Q) methods. The latter is based on the high-accuracy extrapolated *ab initio* thermochemistry (HEAT) model, as used in Ref. 11. The potential energy of the equilibrium structure is set to zero.

method	$\text{CH}_3\text{OH} + \text{OH}^-$	CH_3O^- (H_2O)	$\text{CH}_3\text{O}^- + \text{H}_2\text{O}$
ωB97XD	1.363	0.000	1.071
mHEAT-345(Q)	1.35	0.00	1.00

Table S2: Comparison of harmonic vibrational frequencies (in cm^{-1}) for the equilibrium structure of the CH_3O^- (H_2O) anion, computed using the fitted MSA2 PES function, $\omega\text{B97XD}/\text{AVTZ}$, and fc-CCSD(T)/ANO1 as reported in Ref. 11

$\tilde{\nu}_\alpha$	MSA2 PES	ωB97XD	CCSD(T)
$\tilde{\nu}_1$	54.3	43.8	76.5
$\tilde{\nu}_2$	92.1	111.2	106.6
$\tilde{\nu}_3$	141.7	146.7	149.8
$\tilde{\nu}_4$	350.5	350.6	379.7
$\tilde{\nu}_5$	603.0	559.9	567.4
$\tilde{\nu}_6$	1151.5	1153.5	1144.0
$\tilde{\nu}_7$	1176.3	1177.9	1184.7
$\tilde{\nu}_8$	1181.2	1181.2	1186.8
$\tilde{\nu}_9$	1313.7	1278.0	1325.7
$\tilde{\nu}_{10}$	1459.6	1460.4	1469.0
$\tilde{\nu}_{11}$	1474.2	1470.3	1484.6
$\tilde{\nu}_{12}$	1480.3	1477.9	1494.8
$\tilde{\nu}_{13}$	1697.0	1679.1	1721.2
$\tilde{\nu}_{14}$	2030.3	2112.0	2179.2
$\tilde{\nu}_{15}$	2717.9	2706.9	2708.5
$\tilde{\nu}_{16}$	2748.3	2736.2	2738.1
$\tilde{\nu}_{17}$	2784.2	2776.5	2782.3
$\tilde{\nu}_{18}$	3939.9	3932.4	3869.2

Table S3: Optimized geometry (in xyz format) of the $\text{CH}_3\text{O}^-(\text{H}_2\text{O})$ anion obtained using the MSA2 PES function

1	8			
2	MSA2 PES			
3	H	-2.06358100	0.38414200	0.90022100
4	H	-0.93682300	1.35061100	-0.06453600
5	H	-2.11364200	0.29976900	-0.86560200
6	H	2.04306600	0.28843500	0.81841600
7	H	0.84208400	-0.20543700	-0.08078600
8	C	-1.40351100	0.33828300	-0.00231300
9	O	-0.50829600	-0.67897500	0.02020700
10	O	1.83954100	0.16057300	-0.10693700

Table S4: Optimized geometry (xyz format) of the $\text{CH}_3\text{O}^-(\text{H}_2\text{O})$ anion calculated by the $\omega\text{B97XD}/\text{AVTZ}$ level

1	8			
2	$\omega\text{B97XD}/\text{AVTZ}$			
3	C	-1.413488	0.334595	0.002951
4	O	-0.510128	-0.674738	0.010885
5	H	-2.151495	0.289333	0.842552
6	H	-0.958214	1.351600	0.079158
7	H	-2.045405	0.377341	-0.919978
8	H	0.855910	-0.191656	-0.093030
9	O	1.849097	0.169213	-0.104796
10	H	2.068378	0.210020	0.824882

Table S5: Optimized geometry (in xyz format) of the TS structure obtained from calculations using PES1

1	8			
2	PES1 TS			
3	C	-1.521974183487	-0.281836043022	0.000014212562
4	O	-0.384039621394	0.569809798126	-0.000043119817
5	H	-2.436900051327	0.307785505085	0.000827286400
6	H	-1.518949370792	-0.916935219470	-0.883999696368
7	H	-1.518051930528	-0.917730097457	0.883391078140
8	H	0.697939310835	0.221379086905	-0.000178673717
9	O	1.878117292047	-0.065758580358	-0.000318570178
10	H	1.955202554646	-1.035903449809	0.000287482978

Table S6: Optimized geometry (in xyz format) of the RC structure obtained from calculations using PES1

1	8		
2	PES1	RC	
3	C	-2.060474609404	-0.208374488638
4	O	-0.883601392144	0.587853332970
5	H	-2.946720685445	0.424428653558
6	H	-2.083234173041	-0.856738937206
7	H	-2.093836093060	-0.830609344396
8	H	-0.041941582257	0.127757780296
9	O	2.925500895811	-0.227156281087
10	H	1.975498459490	-0.020785212240

Table S7: Optimized geometry (in xyz format) of the PC structure obtained from calculations using PES1

1	8		
2	PES1	PC	
3	C	-2.296073114156	0.137648880576
4	O	-0.919139033148	0.107242536099
5	H	-2.589459749023	0.501717104649
6	H	-2.706547592957	-0.853805983479
7	H	-2.718547569102	0.789935920896
8	H	3.293513683933	-0.534328473741
9	O	2.963819835459	-0.068245370524
10	H	2.000291183862	-0.024340768648

Table S8: Optimized geometry (in xyz format) of the TS structure obtained from calculations using PES2

1	8		
2	PES2	TS	
3	C	-1.416748129657	-0.284225659340
4	O	-0.313991127701	0.053226519467
5	H	-2.248638927592	0.338443343701
6	H	-1.195215486678	-0.062161191832
7	H	-1.667646646501	-1.332779391054
8	H	0.624090904851	-0.595583446566
9	O	1.600238877906	-0.596979043701
10	H	1.769254535375	0.360869869328

Table S9: Optimized geometry (in xyz format) of the RC structure obtained from calculations using PES2

1	8		
2	PES2	RC	
3	C	-1.832271739778	-0.014983016841
4	O	-0.458400947439	-0.333422253350
5	H	-2.079271895168	0.810715878744
6	H	-2.438128727461	-0.882009183468
7	H	-1.997894971934	0.277434622940
8	H	-0.229678929765	-1.056190792971
9	O	2.229230345183	-0.429503536257
10	H	1.283724944924	-0.168548588597

Table S10: Optimized geometry (in xyz format) of the PC structure obtained from calculations using PES2

1	8		
2	PES2	PC	
3	C	-0.750386086034	-0.273466094211
4	O	-1.600819920314	0.430927836592
5	H	-0.999789076573	-0.238054130085
6	H	0.303419750104	0.103362354742
7	H	-0.794762710336	-1.364073113146
8	H	1.237597011336	-0.883442282662
9	O	2.071177274127	-0.810481547796
10	H	2.549893378220	-1.643070262896